

# International Conference on Microwave & THz Technologies, Wireless Communications and Optoelectronics

*IRPhE' 2024*

## PROGRAM

*Organized by:*

*Institute of Radiophysics and Electronics,  
Armenian National Academy of Sciences*

*Sponsored by:*



**Institute of Radiophysics  
and Electronics,  
Armenian National  
Academy of Sciences**



**National Academy  
of Sciences of the  
Republic of Armenia**



**The RA Ministry of  
Education, Science, Culture  
and Sports. Higher  
Education and Science  
Committee**



**Rohde & Schwarz**

*September 20-21, 2024*

***Venue:* National Academy of Sciences in Yerevan, 24, Marshall Baghramian Ave.**

## **IRPhE' 2024 Main Topics:**

- **Microwave devices, antennas, propagations and remote sensing**
- **THz technique, spectroscopy and applications**
- **Microwave photonics**
- **Wireless communications and related information technologies**
- **Semiconductor and dielectric materials, electronic and optoelectronic devices**

## **Conference Chairs:**

**ArsenHakhoumian (Dr. Sc., Ass. Member NAS RA, IRPhE, Armenia)**

**Tigran Zakaryan (Dr., CEO IRPhE, Armenia)**

## **Program Committee:**

RadikMartirosyan (NAS RA, IRPhE, Armenia)

ArsenHakhoumian (IRPhE, Armenia)

Stepan Petrosyan (IRPhE, Armenia)

Kiejun Lee (SogangUniversity, South Korea)

Robert Minasyan (Sidney University, Australia)

Yuri Avetisyan (YSU, Armenia)

Khachatur Nerkararyan (YSU, Armenia)

## **Organizing Committee:**

Tigran Zakaryan (IRPhE, Chair)

ArsenHakhoumian (IRPhE, Co-chair)

Suren Nersesyan (IRPhE, RA)

Emil Asmaryan (IRPhE, RA)

Hasmik Martirosyan (IRPhE, RA)

20 September, Friday

<b>Microwave &amp; THz Technologies (MW-I)</b>		
<b>Chairman: Prof. Arsen Babajanyan</b>		
09:50-10:00	Opening Speech: Academician of NAS RA, Prof. Radik Martirosyan	
10:00-10:30	Invited talk: Robert Minasian (Sidney University, Australia)	Advances in microwave photonic signal processing and sensing
10:30-10:50	V.Gareyan, N.Margaryan, <u>Zh.Gevorkian</u>	<b>MW1</b> Nanoroughness induced anti-reflection and haze in opaque systems
10:50-11:10	V.A. Vardanyan, <u>M.Ts. Ayvazyan</u>	<b>MW2</b> Terahertz receiver input module
11:10-11:30	Coffee break	
11:30-11:50	<u>H. Vardanyan</u> , A. Hakhumyan, V. Mkhitarian	<b>MW3</b> Application of Bessel beams for radio communication
11:50-12:10	<u>A. Hakhoumian</u> , O. Mahmoodian, H. Vardanyan, V. Mekhitarian	<b>MW4</b> Radially slot leaky-wave antenna for Bessel beams generation
12:30-14:00	Lunch	

<b>Microwave &amp; THz Technologies (MW-II)</b>		
<b>Chairman: Dr. Hovhannes Haroyan</b>		
14:00-14:20	T. Abrahamyan, <u>G. Ohanyan</u> , H.Haroyan, A. Babajanyan, Kh. Nerkararyan	<b>MW5</b> Resonant detection of surface microwaves using dielectric-coated conductive rods coupled with a cut Goubau line
14:20-14:40	<u>A. Movsisyan</u> , B. Minasyan, H. Manukyan, A. Babajanyan	<b>MW6</b> The study of properties of cylindrical metastructures in X-band based on intercomponent coupling and wave interaction
14:40-15:00	Artyom Movsisyan, Hasmik Manukyan, Billi Minasyan, <u>Arsen Babajanyan</u> , Zhirayr Baghdasryan, Kiejin Lee	<b>MW7</b> Characterization of microwave response of the mesh-pattern vs. uniformly-coated Indium-Tin-Oxide indicator for the thermoelastic optical microscope: a comparative analysis
15:00-15:20	<u>T. Hovhannisyan</u> , A. Makaryan, R. Martirosyan	<b>MW8</b> Investigation of nonlinear properties of animal spinal cord in THz range
15:20-15:40	B. Hovhannisyan, T. Hovhannisyan, A. Makaryan, E. Sivolenko, <u>V. Mkhoyan</u>	<b>MW9</b> Statistical analysis of the electroencephalographic signals
15:40-16:00	<u>H. Shahinyan</u> , T. Sargsyan, A. Babajanyan	<b>MW10</b> Strange stars for fixed and density-dependent bag parameter
17:00	Gala dinner	

21 September, Saturday

<b>Semiconductor and dielectric materials, electronic and optoelectronic devices (EL)</b>		
<b>Chairman: Prof. Stepan Petrosyan</b>		
10:00-10:20	S. Petrosyan, <u>A. Musayelyan</u> , A. Tokmajyan, V. Gremenok	<b>EL1</b> CdS thin films formed on flexible plastic substrate by low-temperature chemical bath deposition
10:20-10:40	<u>P. G. Petrosyan</u> , L.N. Grigoryan, L. V. Asryan, N. B. Knyazyan, S. G. Petrosyan	<b>EL2</b> Differential thermal analysis of the crystallization kinetics in perlite-based nanocrystalline glass-ceramics
10:40-11:00	<u>S.G. Petrosyan</u> , A. M. Khachatryan, P.G. Petrosyan	<b>EL3</b> Bi-layer MOS2 phototransistor deposited on a flexible substrate
11:00-11:20	<u>Khachatryan A.M.</u> , Petrosyan S.G., Hovsepyan B.L., Stanchik A.V.	<b>EL4</b> Stoichiometry and phase composition of CdTe thin films prepared by pulsed laser deposition method
11:20-11:40	G. Ayvazyan, <u>H. Dashtoyan</u> , F. Gasparyan, S. Khudaverdyan, L. Matevosyan	<b>EL5</b> Experimental determination of the binding energy of excitons in organometallic perovskite films CH <sub>3</sub> NH <sub>3</sub> PbCl <sub>3</sub> -xI <sub>x</sub> obtained by dual source vacuum thermal evaporation
11:40-12:00	<u>V. Harutyunyan</u> , L. Matevosyan, V. Mkrtychyan, G. Pluzyan, S.Petrosyan, A. Tokmajyan	<b>EL6</b> Investigation of structural and optical properties of CsPbBr <sub>3</sub> films synthesized by single-source vacuum evaporation method
12:00-12:20	<u>V. Plotnikova</u> , M. Nadahovskaya, E. Kalashnikov	<b>EL7</b> Behavior of hydrogen, helium and their isotopes in silicon
12:20-13:30	Lunch	

<b>Microwave &amp; THz Technologies (MW-II)</b>		
<b>Chairman: Dr. Tigran Zakaryan</b>		
13:30-13:50	<u>Y. Sahakyan</u> , Yu. Avetisyan, A. Kirakosyan, A. Makaryan, V. Tadevosyan	<b>MW11</b> Generation of THz radiation in a plane-parallel artificial PPLN crystal with a THz diffraction grating in output
13:50-14:10	<u>T.A. Manukyan</u> , G.Z. Sughyan, H.V. Hambardzumyan, S.G. Eyrarmjyan, B.J.Minasyan, A.K. Aharonyan	<b>MW12</b> Design and preparation of the direction-finding system for using the smart jamming RF signals systems in the 1-6 GHz frequency range
14:10-14:30	<u>E. Sivolenko</u> , A. Hakhoumian, N. Gasparyan, M. Barseghyan, H. Babayan	<b>MW13</b> More accurate and effective monitoring of moving targets in complex environments using “spectral mask” for harmonic signatures using higher-ordered statistics
14:30-14:50	<u>A. Stepanyan</u> , H. Haroyan, A. Hakhoumian	<b>MW14</b> Beam scanning realization by a single electrically small antenna covered by magnetodielectric resonator

14:50-15:10	<u>V.R. Kocharyan</u> , L.Sh. Grigoryan, A.P. Potylitsyn, P.V. Karataev, S.B. Dabagov, A.S.Kubankin, E.Yu. Kidanova, V.N. Antonov, A.V. Vukolov, I.A. Kishin, Y.M. Cherepennikov, M.V. Shevelev, B.A. Grigoryan, A.S. Vardanyan, H.D. Davtyan, A.A. Saharian, H.F. Khachatryan, V.V. Margaryan, A.H. Mkrtchyan	<b>MW15</b> Sub-THz coherent transition and Cherenkov radiation generated at the AREAL accelerator
15:10-15:30	<u>H.V. Baghdasaryan</u> , T.M. Knyazyan, T.T. Hovhannisyanyan, M. Marciniak, T. Baghdasaryan	<b>MW16</b> Metal-dielectric multilayer structure imitating epsilon-near-zero (ENZ) metamaterials: wavelength-scale electromagnetic analysis by the method of single expression
15:30-16:00	Coffee break	
16:00-17:00	Poster session	
17:00-17:15	Closing of IRPhE`2024	

<b>Poster Session</b>	
L. B. Hovakimian	<b>P_EL1</b> The “untakeable” integral in electronic thin film science: calculated?
S. Martirosyan, J. Torikyan	<b>P_MW1</b> Some peculiarities of the Schmitt trigger, inverse problem
A.A. Kuzanyan, V. Nikoghosyan, L. Mheryan, A.S. Kuzanyan	<b>P_MW2</b> Thermoelectric single photon detector for UV radiation with THz count rate
H. Margaryan, V. Abrahamyan, N. Hakobyan, H.Chilingaryan, G. Stepanyan, V. Belyaev, A. Latipov	<b>P_MW3</b> Light beam steering by a sequence of polarization diffraction gratings
N. Gasparyan, A. Hakhoumian, E. Sivolenko, M. Barseghyan	<b>P_MW4</b> SC-DSB signal as a probe signal for testing nonlinearity in electronic circuits
D. Baghdasaryan, A. Makaryan, V. Mekhitarian, A. Poghosyan, Y. Sahakyan	<b>P_MW5</b> Generation of THz pulses in the transparent ferromagnetic materials by optical rectification of ultrafast laser pulses
A. S. Nikoghosyan, V. R. Tadevosyan, H. A. Parsamyanyan, A. A. Poghosyan	<b>P_MW6</b> Terahertz radiation in a nonlinear crystal partially filling a parallel-plate waveguide
A. G. Ghulyan, N. D. Yezakyan, H. Arakelyan	<b>P_MW7</b> Existing radio sources for antenna measurements
N.D. Yezakyan	<b>P_MW8</b> Design and analysis of quadcopter classical controller
L. Gevorgyan	<b>P_MW9</b> Tunable terahertz bandstop filter based on bilayer metasurface
Grigor Tsaturyan	<b>P_MW10</b> Spectral emission mask measurement improvement technique for IEEE 802.15.4z ultra-wideband devices
Samvel Antonyan	<b>P_MW11</b> System design and implementation of multiprobe near field antenna measurements
H.L. Babayan, N.G. Poghosyan, S.T. Sargsyan, T.V. Zakaryan	<b>P_MW12</b> Moving target indication as a radar cross section rapid estimate

**Microwave & THz technologies**  
**(MW)**

## **Nanoroughness induced anti-reflection and haze in opaque systems**

V.Gareyan<sup>1</sup>, N.Margaryan<sup>1</sup> and Zh.Gevorkian<sup>1,2</sup>.

<sup>1</sup>*Alikhanyan National Laboratory, Alikhanian Brothers Brothers str. 2, 0036 Yerevan, Armenia*

<sup>2</sup>*Institute of Radiophysics and Electronics, Alikhanian Brothers str. 1, 0203 Ashtarak, Armenia*

We have studied specular and diffuse scattering of light from a weakly rough opaque surface. A theory is developed that utilizes new modified boundary conditions. They significantly change the results both for specular and diffuse scattered intensities. An anti-reflection is predicted in the wavelength region where light penetration depth into medium is of order of roughness root mean square height. This phenomenon is observed experimentally for nano-roughened *Si* films in the 300-400nm region. Angular and polarization dependences of diffuse scattered (haze) light are revealed. It is shown that the haze is mainly p-dominated and is directed around the surface normal independent of the incident angle.

## Terahertz receiver input module

V.A. Vardanyan<sup>1</sup>, M.Ts. Ayvazyan<sup>2</sup>

<sup>1</sup> Russian-Armenian University

<sup>2</sup> National Polytechnic University of Armenia

Currently, the vast majority of radio engineering systems use superheterodyne type radio receivers which is due to their high sensitivity and selectivity in the neighboring channel. In the terahertz range the losses make a significant contribution to the noise factor of the receiver, and therefore, considerable attention is paid to the development of quasi-optical devices.

Microwave mixers based on diodes with a Schottky barrier used in the terahertz range require increased local oscillator power ( $\geq 10$  mW), significant losses in the local oscillator channel significantly limit the use of such devices.

Therefore, the use of an interferometric addition circuit, for superheterodyne receivers with ultra-high intermediate frequency  $f_{IF} = (2 \div 10)$  GHz, is of significant interest. This could be a Mach-Zehnder interferometer which contains two dielectric beam splitters, as well as two angle bends.

Half-wave interferometer provides local oscillator noise suppression, similar to the balanced mixer circuit that is widely used in microwave receivers. However, in contrast to traditional balanced circuits, the operating efficiency of which depends on the identity of two mixing diodes, in the case under consideration, a high degree of local oscillator noise suppression (at least 10 dB) is achieved when using one mixing diode, and the receiver noise is determined mainly by noise intermediate frequency amplifier.

The interferometric addition scheme can be significantly improved by using a polarization Michelson interferometer, based on metal dielectric oversize waveguide which can significantly reduce the size of the device. In this case, the device (Fig. 1) contains polarizing gratings 1, 2 and 5, as well as dihedral 90° corner reflectors 3 and 4, and the elements of the gratings 1 and 5 are oriented in the same way, and grating 2, the dihedral reflectors are rotated around the waveguide axis by 45° relative to grid elements 1 and 5.

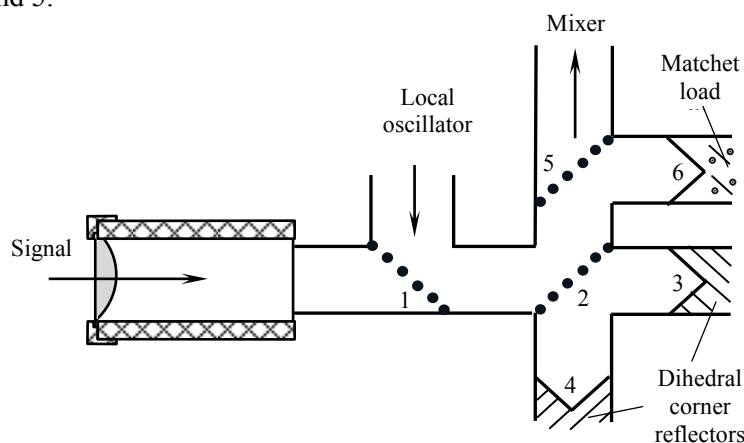


Fig. 1. Input part of a terahertz receiver based on a Michelson interferometer

As a result, in contrast to the Mach-Zehnder interferometer, the path difference equal to half the wavelength of oscillations of the intermediate frequency  $L = \lambda_{IF}/2$ , in this case, is realized with half the length of the oversize waveguide segment.

## Application of Bessel beams for radio communication

H. Vardanyan<sup>1</sup>, A. Hakhumyan<sup>1</sup>, V. Mkhitarian<sup>2</sup>

<sup>1</sup>*Institute of Radiophysics And Electronics Ashtarak, Armenia 0203*

<sup>2</sup>*Physical research institute, Ashtarak, Armenia 0203*

Bessel beams are considered by some observations to be much more stable to diffraction than the usual linearly polarized plane wave.

As a result of these experiments, it was more obvious. Objects with different symmetry and sizes were used as a barrier, in which case the Bessel beams showed stability. It is also important to note that the size of the barrier plays a significant role in signal recovery, as the size of the barrier increases, the extinction also increases. However, if the obstruction of the main path is completely covered by the first Fresnel zone, there is no significant attenuation of the signal, if not certainly an improvement.

In the previous work, a flat disk with a diameter of 11.2 cm was used as a barrier to check the stability against barriers and an improvement of the signal from -46 dB to -41 dB was noticed. Figure 1 shows the phenomenon, where a red line separates free space extinctions from extinctions caused by the displacement of the sphere. In the range above the red line, the barrier fully covers the first Fresnel zone and partly the second.

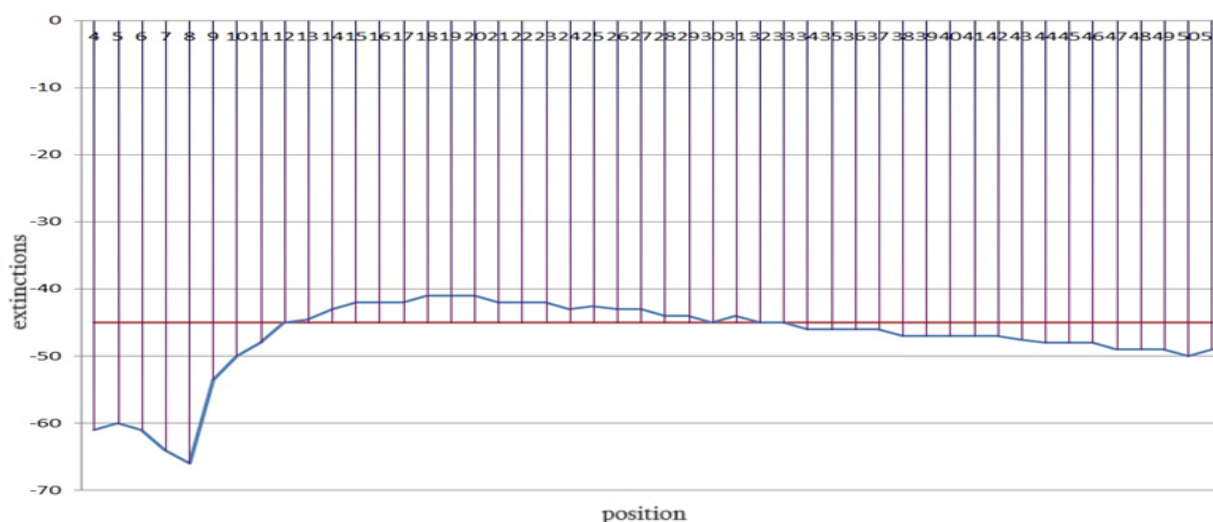


Figure 1. The effect of the barrier on the signal

The goal of the research was to create Bessel antennas, which were used in our measurements. A single wire and a Fresnel lens were used for the reception. As a result, we got a  $J_1$  Bessel beam, which has radial polarization. Measurements were made at a frequency of 30 GHz, and a ZNA vector network analyzer with a frequency range of 10 MHz - 43.5 GHz was used for the measurement. 3D modeling was also performed and compared with the obtained results.

## **Radially slot leaky-wave antenna for Bessel beams generation**

A. Hakhoumian<sup>1</sup>, O. Mahmoodian<sup>1</sup>, H. Vardanyan<sup>1</sup>, V. Mekhitarian<sup>2</sup>

<sup>1</sup>*Institute of Radiophysics and Electronics of NAS RA, Alikhanian Brothers str. 1, Ashtarak, 0203, Armenia*

<sup>2</sup>*Institute of Physical Research of NAS RA, Ashtarak, 0204, Armenia*

The radial line resonator based slotted antenna is studied for generation of first-order Bessel beams over a wide frequency range. The analytical methods to determine resonant condition and resonant frequencies of short-circuit radial line was developed. The resonant frequencies experimental results are in good agreement with calculation results. The far field radiation pattern of radial slot antenna is measured and plotted for different distances. As is expected, the radiation pattern of antenna is conical which has no radiated power in the direction of  $Z$  which includes two main beams on both sides of  $Z$ -axis which can be defined by the first kind of Bessel function. The far field radiation pattern of antenna is plotted after focusing by a parabolic reflector due to its radially symmetric shape. The power of reflected beam from parabolic is more strength and also the main lobes of plotted radiation pattern become closer to the  $Z$ -axis. In addition, the transversal field distribution keep behavior at the distance up to  $100\lambda$ .

## **Resonant detection of surface microwaves using dielectric-coated conductive rods coupled with a cut Goubau line**

T. Abrahamyan, G. Ohanyan, H. Haroyan, A. Babajanyan, Kh. Nerkararyan

*Institute of Physics, Yerevan State University, Yerevan, Armenia*

This paper explores a novel approach to mitigate dielectric and Ohmic losses in microwave frequencies and minimize signal dispersion using surface waves on wires with circular cross-sections, as discovered by Sommerfeld. While the extensive radial extension of Sommerfeld surface waves initially poses challenges due to the requirement of large isolated areas around conductors to avoid field distortion, Goubau's discovery offers a solution. By coating wires with dielectric layers, known as Goubau lines, lateral confinement of surface waves can be significantly enhanced, expanding their range of applications. These communication elements offer numerous advantages including low losses, dispersion, and simplified fabrication processes, making them ideal for ultra-wideband applications. This study investigates the resonant properties of coupled conductive rods, demonstrating their effectiveness as resonators for surface radial electromagnetic waves at microwave frequencies. The formation of standing waves is influenced by the unique distribution of radial surface waves, ensuring noticeable reflections from rod edges. Furthermore, coupling with plane microwaves polarized along the rod axis is facilitated by the relatively weak electric field component of surface waves formed along the rod axis. The integration of double cylindrical conductive resonators with a cut Goubau line is examined, revealing sharper narrow-band resonances compared to a single rod configuration. Such resonances hold promise for practical applications as sensitive systems for monitoring ambient conditions.

## **The study of properties of cylindrical metastructures in X-band based on intercomponent coupling and wave interaction**

A. Movsisyan, B. Minasyan, H. Manukyan, A. Babajanyan

*Yerevan State University, 0025, Alex Manoogian str.1, 0025, Yerevan, Armenia*

In this work, for the first time, results are presented where the cylindrical system is multi-component, and inside the cylinder is not one rod but two or more. This multi-component system increases the resonances and produces multiple regions on the spectrum when the number of rods exceeds two. The physical nature of resonances, which do not occur for the same reason, is also explained. Also, this system can be enjoyable from the sensory point of view because Fano resonance systems are very delicate and controllable. The deviation of the resonance depending on the change in the dielectric permeability of the air was studied. It was found that this system can serve as a relatively sensitive sensor: in the case of a deviation of the dielectric permeability of air of the order of  $10^{-2}$ , the resonances deviate by 50 MHz. Furthermore, this structure can serve as a component in wireless communication.

**Characterization of microwave response of the mesh-pattern vs. uniformly-coated Indium-Tin-Oxide indicator for the thermoelastic optical microscope: a comparative analysis**

Artyom Movsisyan<sup>1</sup>, Hasmik Manukyan<sup>1</sup>, Billi Minasyan<sup>1</sup>, Arsen Babajanyan<sup>1</sup>,  
Zhirayr Baghdasryan<sup>2</sup>, Kiejin Lee<sup>2</sup>

<sup>1</sup>*Institute of Physics, Yerevan State University, Yerevan, Armenia*

<sup>2</sup>*Department of Physics, Sogang University, Seoul, Korea*

The microwave absorption characteristics of Hilbert-shape mesh-patterned ITO structure were examined using thermoelastic optical microscope (TEOM). Specifically, the study investigated how the distribution of the microwave electromagnetic field changes when comparing ITO indicators with mesh-pattern to those with uniform structure within the 8-12 GHz range. The findings demonstrate that by introducing certain dispersion anisotropy in the absorbing layer of the ITO indicator, both the sensitivity of the microscope and the ability to image different spatial components of the incident microwave field separately can be significantly enhanced. These results offer valuable insights for optimizing the microwave absorption process in the development of high-performance thermoelastic devices based on ITO films.

## Investigation of nonlinear properties of animal spinal cord in THz range

T. Hovhannisyan<sup>1</sup>, A. Makaryan<sup>1</sup>, R. Martirosyan<sup>1,2</sup>

<sup>1</sup>*Yerevan State University, Alex Manoogian str. 1, 0025 Yerevan, Armenia*

<sup>2</sup>*Institute of Radiophysics and Electronics, Alikhanian Brothers str. 1, 0203 Ashtarak, Armenia*

In the present work the electrodynamic properties of a system consisting of parallel arranged animal spinal cord nerve fibers in the terahertz range (0.1 - 3 THz) by time domain spectrometer are experimentally investigated.

The measurements showed that in the absence of external influences, the electrodynamic parameters of the spinal cord sample (refractive index, absorption) remain mostly unchanged for a long time (up to several hours). Significant changes in the parameters are observed when an external constant voltage is applied to the sample through electrodes placed parallel to the nerve fibers. These changes are highly significant when the electric field vector of the THz radiation is oriented parallel to the nerve fibers. In particular, clearly noticeable resonances appear, which smoothly shift to lower frequencies over time (5 minutes), and then the change of parameters ceases. After removing the external voltage, the parameters of the sample slowly return to their initial values (within about an hour).

A model was proposed, according to which the application of external voltage leads to the opening of the Ranvier nodes of the nerve fibers, as a result of which the nerve fibers of the spinal cord turn into a kind of nonlinear conductors, and the whole sample into a diffraction grating. Computational modeling of the interaction of THz radiation of the spinal cord sample was performed, the results of which are in good agreement with the experimentally obtained results.

## Statistical analysis of the electroencephalographic signals

B. Hovhannisyan, T. Hovhannisyan, A. Makaryan, E. Sivolenko, V. Mkhoyan

*Yerevan State University, Alex Manoogian str. 1, 0025 Yerevan, Armenia*

In the study of signals (especially biosignals), along with spectral analysis, bispectral analysis is often used. Despite the fact that bispectral analysis requires relatively large computing resources and appropriate software, it can provide additional valuable information about the signal that cannot be obtained by spectral analysis alone.

In this work, radio signals received from the brain (in the frequency range up to several tens of megahertz) were recorded using various sensors and their statistical (in particular, spectral and bispectral) analysis was performed in the LabVIEW environment using the Advanced Signal Processing Toolkit.

Research has demonstrated that bispectral analysis can identify spectral components within biosignals that are statistically related to each other and are also somewhat correlated with a person's mental and physical states.

Based on the results of spectral and bispectral analyses of signals recorded with sensors, a system was developed which pre-filters non-informative components of signals, due to which disturbances are reduced, and therefore the effectiveness of the statistical analysis of the signals is increased.

## Strange stars for fixed and density-dependent bag parameter

H. Shahinyan<sup>1</sup>, T. Sargsyan<sup>2</sup>, A. Babajanyan<sup>1</sup>

<sup>1</sup>*Yerevan State University, 0025, Alex Manoogian str.1, 0025, Yerevan, Armenia*

<sup>2</sup>*Synopsys Armenia CJSC, Arshakunyats Ave. 41, 0026, Yerevan, Armenia*

Strange stars with maximal masses, more than the values of recently precisely measured masses of two radio pulsars: *SRJ0740 + 6620*, with the mass  $2.14M_{\odot}$ , and *PSRJ2215 + 5135*, with the mass  $2.27M_{\odot}$ , have been studied. For the examination of strange quark matter (*SQM*), the bag model, developed in Massachusetts Technological Institute was chosen. The observed bag model depends on vacuum pressure  $B$ , quark-gluon interaction constant  $\alpha_c$ , and strange quark mass  $m_s$ . Since the transition to *SQM* state takes place at the energy density, not exceeding double density in atomic nuclei, neutron stars with small mass and configuration, consisting of *SQM*, form one family in the dependence curve of the mass  $M$ , of the equilibrium super-dense configurations, on the energy central density  $\rho_c$  (curve  $M(\rho_c)$ ). The state equation of strange quark matter was studied for two cases: when the vacuum pressure was constant and depended on baryon density  $B(n_b)$ . For constant vacuum pressure, the state equation of *SQM* leads to the maximal mass of the equilibrium quark configurations  $M_{max}$ , heavier than the mentioned radio pulsars. For such configurations, the values of mass, radius, the entire number of baryons, and redshift from the strange star surface were calculated, depending on the energy central density  $\rho_c$ . According to the obtained state equations, these two radio pulsars can be possible candidates for the strange stars. For comparison, integral parameters were calculated for stars corresponding to the second case. Gaussian parameterization  $B(n)$  is considered here. Such dependence is explained by the fact that the concentration of quark matter increases from the star's surface to the center. In this case, the maximum masses are smaller than  $2M_{\odot}$ . It means that the fixed vacuum pressure describes the *SQM* state more accurately. On the other hand, if we consider the rotation of the stars, the second case could also provide large masses.

## **Generation of THz radiation in a plane-parallel artificial PPLN crystal with a THz diffraction grating in output**

Y. Sahakyan, Yu. Avetisyan, A. Kirakosyan, A. Makaryan, V. Tadevosyan

*Yerevan State University, Alex Manoogian str. 1, 0025 Yerevan, Armenia*

Optical rectification (OR) of femtosecond laser pulses in periodically poled lithium niobate (PPLN) crystals is a simple and widely used method to generate narrowband THz pulses. Artificial periodically poled LN crystals are also widely used.

In this case, THz radiation occurs at a Cherenkov angle, therefore, to avoid complete internal reflections, triangular crystals with an output front tilted at a Cherenkov angle are used. The use of triangular shaped crystals leads to a decrease in the efficiency of THz generation.

Moreover, in a triangular crystal, the propagation lengths of individual pump beamlets are different, leading to a lower quality of the generated THz beam and, consequently, to a poor focusing. This problem can be overcome by the application of the plane-parallel form of the artificial periodically poled nonlinear crystal.

However, in the proposed scheme, THz radiation generation occurs simultaneously in two directions, i.e. at Cherenkov angles relative to the propagation of the pump pulse. For this reason, in this paper, it is proposed to use a THz diffraction grating as an output communication element.

The passage of THz radiation generated by a diffraction grid installed at the outlet of a nonlinear crystal from the crystal into the air was simulated in the COMSOL Multiphysics environment.

It has been shown that with the correct choice of the diffraction grating, a symmetrical THz burst is obtained at the output and the efficiency of the transition from crystal to air can be received up to 50%.

## **Design and preparation of the direction-finding system for using the smart jamming RF signals systems in the 1-6 GHz frequency range**

T.A. Manukyan<sup>1,3</sup>, G.Z. Sughyan<sup>1</sup>, H.V. Hambardzumyan<sup>1,3</sup>, S.G. Eyranyan<sup>1,2</sup>, B.J. Minasyan<sup>1,5</sup>, A.K. Aharonyan<sup>1,4</sup>

*1 Russian-Armenian (Slavonic) University, Hovsep Emin str. 123, 0051 Yerevan, Armenia*

*2 "SE Tech" LLC, Bagrevandi St., 21/1, 0062 Yerevan, Armenia*

*3 YEA Engineering, Bagrevandi St., 21/1, 0062 Yerevan, Armenia*

*4 Yerevan Telecommunication Research Institute, Dzorap str.26, 0056 Yerevan, Armenia*

*5 Yerevan State University, Alek Manukyan str.1, 0025 Yerevan, Armenia*

The rapid development of wireless communication technologies has required the use of advanced methods of protection and management of the radio frequency (RF) spectrum. Jamming is the most important method of interrupting unauthorized or malicious communications, but traditional methods are often inaccurate and can interfere with legitimate users.

The purpose of this work is to design and development of a smart RF jamming system that includes an adaptive direction-finding component to improve accuracy and minimize unintended interference.

The proposed system uses an amplitude comparison method that measures the strength of a signal received by several spatially spaced antennas. Adaptive algorithms allow real-time correction of the direction of the suppressed signal to the target source.

The experimental results demonstrate the effectiveness of the system in accurately targeting and suppressing certain signals, minimizing interference to non-targeted messages. The system demonstrates significant improvements in efficiency and strategic application in scenarios such as electronic warfare, security operations and the protection of critical infrastructure.

The developed smart RF jamming system using adaptive direction finding represents significant progress in radio frequency spectrum management and safety. It is a practical and effective tool for precise and effective jamming in an era of sophisticated wireless communications.

## **More accurate and effective monitoring of moving targets in complex environments using “spectral mask” for harmonic signatures using higher-ordered statistics**

E. Sivolenko<sup>1</sup>, A. Hakhoumian<sup>1,2</sup>, N. Gasparyan<sup>1</sup>, M. Barseghyan<sup>1</sup>, H. Babayan<sup>2</sup>

<sup>1</sup>*Yerevan State University, Alex Manoogian 1, Yerevan, Armenia*

<sup>2</sup>*Institute of Radiophysics and Electronics, Alikhanian Brothers str. 1, 0203 Ashtarak, Armenia*

In the field of signal processing and target detection, bispectral analysis provides a robust framework for identifying and characterizing non-linear interactions and harmonic relationships in time series data. This paper presents an innovative approach to bispectral analysis customized for moving targets, utilizing spectral masks to improve the detection of harmonic frequencies.

Our method involves the creation of a spectral mask that selectively amplifies the desired harmonics within the bispectrum, effectively reducing noise and other irrelevant signals. This targeted approach enhances the resolution and clarity of harmonic signatures, facilitating improved tracking and characterization of moving targets. We validate the effectiveness of our approach through simulations and real-world scenarios, demonstrating significant enhancements in target detection performance and frequency resolution compared to traditional bispectral analysis methods.

The proposed technique paves the way for advanced signal processing applications, particularly in radar and sonar systems, where precise target tracking and classification are crucial. By refining the bispectral analysis process and concentrating on harmonic frequencies, our method contributes to more accurate and efficient monitoring of moving targets in complex environments.

## Beam scanning realization by a single electrically small antenna covered by magnetodielectric resonator

A. Stepanyan<sup>1</sup>, H. Haroyan<sup>1,2</sup>, A. Hakhoumian<sup>1,2</sup>

<sup>1</sup> Institute of Radiophysics and Electronics, Alikhanian Brothers str. 1, 0203 Ashtarak, Armenia

<sup>2</sup> Yerevan State University, Alex Manoogian 1, Yerevan, Armenia

Beam scanning antennas are widely used across various applications. One instance is phased array utilizes beamformers and are characterized by their complex structures. This paper presents an innovative beam scanning technique, implemented in an electrically small microstrip patch antenna covered by a hemispherical magnetodielectric resonator. Magnetodielectric resonator impacts the performance of the microstrip patch antenna by being positioned in its reactive near-field region (Figure 1), which is designed to operate at a frequency of 13 GHz.

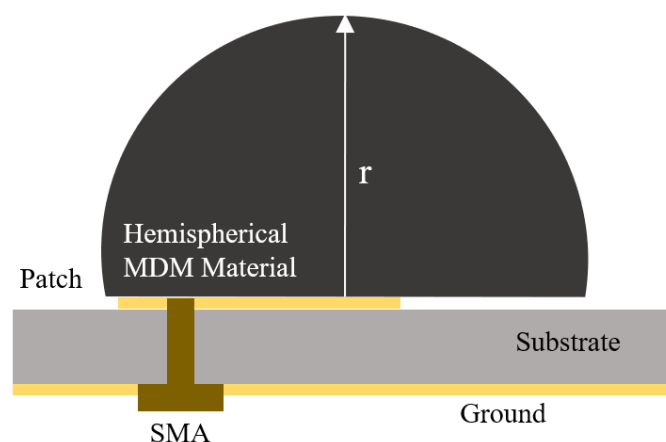


Figure 1. Schematic view of microstrip patch antenna covered by hemispherical magnetodielectric resonator

The designed antenna exhibits a reduced frequency range (2.4 GHz), introducing the concept of an electrically small antenna. The impedance and modal distribution of the antenna are changed by adjusting the position of the magnetodielectric (MDM) resonator relative to the microstrip antenna. The beam scanning effect is introduced as a function of frequency, differing from conventional phased array operations by controlling the field distribution within a single antenna. Beam scanning occurs due to the excitation of higher modes of the resonator at different frequencies with different mode distributions. Additionally, at large scanning angles, the antenna maintains a low side lobe level, which extends the range of the beam scanning capability.

*Keywords: beam scanning, electrically small antenna, hemispherical magnetodielectric resonator.*

### References

1. Igor Sushencev Alexey A. Shcherbakov et al Superdirective dielectric spherical multilayer antennae, 2019 IEEE International Conference on Microwaves, Antennas, Communications and Electronic Systems (COMCAS), 2019.
2. Amelia Buerkle, Kamal Sarabandi A Wide-Band, Circularly Polarized, Magnetodielectric Resonator Antenna, IEEE Transactions on Antennas and Propagation, 53(11), pp3436-3442, 2005.
3. Haozhan Tian, Kirti Dhawaj, Li Jun Jiang, Tatsuo Itoh Beam Scanning Realized by Coupled Modes in a Single-Patch Antenna Best, IEEE ANTENNAS AND WIRELESS PROPAGATION LETTERS, VOL. 17, NO. 6, JUNE 2018.

## Sub-THz coherent transition and Cherenkov radiation generated at the AREAL accelerator

V.R. Kocharyan<sup>1</sup>, L.Sh. Grigoryan<sup>1</sup>, A.P. Potylitsyn<sup>2</sup>, P.V. Karataev<sup>3</sup>, S.B. Dabagov<sup>4</sup>, A.S. Kubankin<sup>5</sup>, E.Yu. Kidanova<sup>5</sup>, V.N. Antonov<sup>3</sup>, A.V. Vukolov<sup>2</sup>, I.A. Kishin<sup>5</sup>, Y.M. Cherepennikov<sup>1,2</sup>, M.V. Shevelev<sup>2</sup>, B.A. Grigoryan<sup>6</sup>, A.S. Vardanyan<sup>6</sup>, H.D. Davtyan<sup>6</sup>, A.A. Saharian<sup>1</sup>, H.F. Khachatryan<sup>1</sup>, V.V. Margaryan<sup>1</sup>, A.H. Mkrtchyan<sup>1</sup>

<sup>1</sup>*Institute of Applied Problems of Physics of NAS RA, 25 Hr. Nersisyan Str., Yerevan 0014, Armenia*

<sup>2</sup>*Tomsk Polytechnic University, Lenin Ave. 30, Tomsk 634050, Russia*

<sup>3</sup>*John Adams Institute at Royal Holloway, University of London, Egham, Surrey, TW20 0EX, UK*

<sup>4</sup>*INFN Laboratori Nazionali di Frascati, Via E. Fermi 40, I-00044 Frascati (RM), Italy*

<sup>5</sup>*Belgorod State National Research University, 85 Pobedy str., Belgorod 308015, Russia*

<sup>6</sup>*CANDLE SRI, 31 Acharyanst., Yerevan 0022, Armenia*

The results of an experimental study of the spectral angular distribution of coherent transition and Cherenkov radiation in the sub-terahertz frequency range are presented. As targets, a thin silicon plate with an aluminium coating and a cylindrical Teflon resonator were used. The AREAL linear accelerator, with an energy of 3.6 MeV and located at the CANDLE Synchrotron Research Institute in Yerevan, served as the electron source. Radiation was recorded using SBD (Schottky Barrier Diode) detectors, designed for frequencies ranging from 33.5 to 50 GHz, 60 to 90 GHz, and 90 to 140 GHz. The obtained results were compared with previous experimental data and theoretical estimates. THz and sub-THz radiation generated by ultra relativistic charged particles can be used for development of intense sources of photons as well as for particle beam diagnostics.

The work was partially supported by the Science Committee of RA, in the frames of the research project № 21AG-1C069.

## Metal-dielectric multilayer structure imitating epsilon-near-zero (ENZ) metamaterials: wavelength-scale electromagnetic analysis by the method of single expression

H.V. Baghdasaryan<sup>1</sup>, T.M. Knyazyan<sup>1</sup>, T.T. Hovhannisyan<sup>1</sup>, M. Marciniak<sup>2</sup>,  
T. Baghdasaryan<sup>3</sup>

<sup>1</sup>National Polytechnic University of Armenia, 105, Terian Str., 0009 Yerevan, Armenia

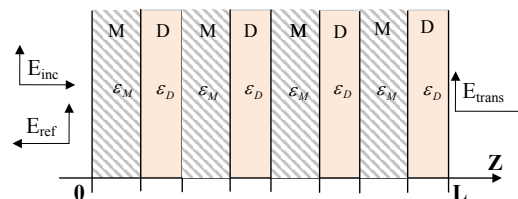
<sup>2</sup>National Institute of Telecommunications, 1. Szachowa Str., 04-894 Warsaw, Poland

<sup>3</sup>Vrije Universiteit Brussel (VUB), Pleinlaan 2, 1050 Elsene, Belgium

In the realm of photonics electromagnetic research deals with materials that allow waves to propagate freely through such media. Electromagnetically these materials, such as dielectrics and semiconductors, are described with positive permittivity, which is equal or more than one. Meanwhile, in the field of plasmonics materials with negative permittivity are being considered and this is usually achieved using metals.

Recently, media and materials where the permittivity is close to zero or so called epsilon-near-zero (ENZ) materials have attracted wide research attention, owing to their remarkable physical properties and novel electromagnetic (EM) phenomena associated with them [1]. Such unusual EM properties are being achieved by metamaterials, which are artificially engineered materials with properties designed to control and manipulate light at the nano-scale level. Prospective applications of ENZ metamaterials include but are not limited to: an effective antenna substrate, plasmonic materials, effective modulators, booster of thermal emission, et al. The growing wide area of ENZ metamaterials' application dictates correct EM analysis of optical characteristics that will be useful for deep understanding the phenomena of EM wave interaction with different ENZ metamaterials. Correct wavelength-scale EM computer modelling is a necessary initial step for designing any nano-structures, before their costly fabrication process. For numerical modelling we are using the method of single expression (MSE), as it proved its ability to solve different related multi-boundary problems: linear and nonlinear [2]. The MSE is a frequency-domain method and gives steady-state solution of different multi-boundary problems for normal and oblique incidence of TE and TM waves on multilayer structures consisting of metal, semiconductor and dielectric layers.

The numerical modelling is done for the following structure at the plane wave normal incidence from the left on a metal-dielectric multi-nano-layer structure, where permittivities are  $\epsilon_D > 0$ ,  $\epsilon_M < 0$ ,  $\epsilon_D = |\epsilon_M|$ :



The performed analysis gives information regarding distributions of electric and magnetic fields and Poynting vector of optical wave within the ENZ structure and in surround media. This type of information is useful for understanding the physics and practical realization of ENZ structures. In the result of numerical analysis necessary information regarding the thicknesses of metal and dielectric nano-layers are obtained.

References:

- [1] J. Wu, Z.T.A. Xie, Y. Sha, H.Y. Fu, Q. Li, "Epsilon-near-zero photonics: infinite potentials" *Photonics Research*, 9, No. 8 pp. 1616-1644 (2021) <https://doi.org/10.1364/PRJ.427246>
- [2] H.V. Baghdasaryan, T.M. Knyazyan, T.T. Hovhannisyan and M. Marciniak. Metal-dielectric Multilayer Structure Supporting Surface Plasmons: electromagnetic modelling by the Method of Single Expression" *Optical and Quantum Electronics*, vol. 47, Issue 1, 2015, pp. 3-15 <https://doi.org/10.1007/s11082-014-0003-3>

## **Some peculiarities of the Schmitt trigger, inverse problem**

S. Martirosyan, J. Torikyan

*Institute of Radiophysics and Electronics, Alikhanian Brothers str. 1, 0203 Ashtarak, Armenia*

New equations have been derived for solving the inverse problem of calculating Schmitt's inverting and non-inverting classic triggers, in which the input threshold voltages are known as the main and invariant parameters. Some features of these equations have been revealed. All the unknown values of the trigger scheme were calculated: the parameters of active and passive elements, the values of their power supply voltages and the polarity were justified. Equations for calculating the relative errors of the threshold voltages were derived. Dependences of relative errors of two input threshold voltages (high, low) on trigger output voltages and their relative errors were calculated. The effect of output voltage errors on threshold voltage errors was evaluated. On the basis on the calculation tables, graphs of the dependence of the relative errors of two input threshold voltages of the output voltages were constructed. They are straight lines passing through the point of intersection of the coordinate axes. This allows one to plot these curves on a graph with just one selection of output voltage pairs and just one calculation of the relative errors of the two threshold voltages. After constructing that curve, it is possible to select the pair of output voltages that will provide the smallest error in the threshold voltages. The selection of all parameters and components of the inverting and non-inverting classical triggers is justified. Solutions have been proposed to simultaneously reduce the relative errors for both thresholds in the conditions of the existing errors of the output voltages. With them a new Schmitt trigger can be calculated, avoiding the errors that occur during the calculation of the direct problem, when the choices of the circuit parameters are not justified. Reasonable selection of the technical parameters of the triggers with the proposed methods makes it possible to increase the quality of the triggers.

## Thermoelectric single photon detector for UV radiation with THz count rate

A.A. Kuzanyan, V. Nikoghosyan, L. Mheryan, A.S. Kuzanyan

*Institute for Physical Research of NAS of Armenia, Ashtarak-2, 0204, Ashtarak, Armenia*

Single photon detectors are the most sensitive devices for detecting radiation across a wide range of wavelengths. Single photon detectors in the UV range are widely used in various fields, such as quantum electronics, spectroscopy, astronomy, space astronomy, biology, security, lowlight imaging, and other scientific and technological fields. The UV spectral range is rich with atomic and molecular lines, which hold significant importance in the study of diverse objects. In astrophysics, these objects include planets, satellites, comets, stars, black holes, and galaxies. Numerous types of photon counting detectors, utilizing various physical effects have been developed, in particular photomultiplier tubes, avalanche photodiodes, and superconducting nanowire single-photon detectors. The concept of a thermoelectric single-photon detector was introduced in 2000.

Here we present the results of modeling and simulation of heat propagation processes in thermoelectric sensors after absorption of single UV photons with energies ( $E$ ) in the range from 7.1 to 124 eV. Thermoelectric multilayer sensors with an operating temperature of 1 K consist of a tungsten absorber, a thermoelectric layer of  $\text{La}_{0.99}\text{Ce}_{0.01}\text{B}_6$ , a tungsten heat sink and a dielectric substrate of  $\text{Al}_2\text{O}_3$ . Modeling and simulation of heat transfer processes in thermoelectric sensors with different layer thicknesses and surface areas was carried out using the three-dimensional matrix method for differential equations based on the equation of heat propagation from a limited volume. The temporal dependencies of the temperature at various points in the detection pixels and the average temperature of the layers' surfaces were calculated.

After the absorption of a photon in the sensor absorber, a temperature difference is formed at the boundaries of the thermoelectric layer with the absorber and heat sink, resulting in the formation of a thermopower, which is the sensor signal. The main signal parameters, such as the maximum of average temperature difference on the thermoelectric layer ( $\Delta T_{\text{am}}$ ), time to reach maximum ( $t_m$ ), time of signal decay to the background level ( $\tau$ ), full width at half maximum, and signal power, were determined. The phonon noise, Johnson noise, and the total noise equivalent power of the sensor with a surface area ( $A$ ) of 1 and 4  $\mu\text{m}^2$ , absorber thicknesses ( $d_1$ ) ranging from 40 to 500 nm, and thermoelectric layer thicknesses ( $d_2$ ) ranging from 10 to 100 nm were calculated. The data obtained show how the signal-to-noise ratio (SNR) depends on the energy of the absorbed photon, the geometry of the sensor, and the bandwidth of the signal measurement. The following basic patterns were established.

Parameter  $\Delta T_{\text{am}}$  increases linearly with higher photon energy. Similarly, the parameter  $\tau$  also increases with increasing photon energy, and for the same energies, as well as  $\Delta T_{\text{am}}$ , is larger for the sensor with a surface area of 1  $\mu\text{m}^2$ .

In the case of absorbing photons with an energy of 124 eV the  $\Delta T_{\text{am}}$  decreases, and the  $\tau$  increases linearly with absorber thickness increasing. For the same absorber thickness, both parameters are larger for the detection pixel with a surface area of 1  $\mu\text{m}^2$ .

It was observed that the SNR exceeds unity multiple times for the absorption of photons of all considered energies in the detection pixel with a surface area of 1  $\mu\text{m}^2$ .

The parameter FWHM does not depend on the energy of the absorbed photon or the surface area of the detection pixel. For the detection pixel with layer thicknesses of  $d_1 = 40$  nm and  $d_2 = 100$  nm, the FWHM is determined to be 0.196 ps. Corresponding count rate of thermoelectric sensor will be equal to 5.1 THz.

The SNR is greater than unity for all values of surface area and photon energy, except for  $A = 4$   $\mu\text{m}^2$  and  $E = 7.1$  eV. The highest SNR values were obtained at  $E = 124$  eV and are equal to 162 and 462 for  $A = 4$   $\mu\text{m}^2$  and  $A = 1$   $\mu\text{m}^2$ , respectively.

The patterns obtained allow us to propose an optimal design for detection pixels when using thermoelectric sensors in specific applications.

The work was supported by the Higher Education and Science Committee of RA, as part of research project No. 21T-1C088.

## Light beam steering by a sequence of polarization diffraction gratings

H. Margaryan<sup>1</sup>, V. Abrahamyan<sup>1</sup>, N. Hakobyan<sup>1</sup>, H.Chilingaryan<sup>1</sup>, G. Stepanyan<sup>1</sup>,  
V. Belyaev<sup>2</sup>, A. Latipov<sup>2</sup>

<sup>1</sup>*Yerevan State University, Alex Manoogian str. 1, 0025 Yerevan, Armenia*

<sup>2</sup>*Federal State University of Education, Radio str., 10A, 105005 Moscow, Russia*

Driving a position of light beam, i.e. light beam steering, is a rapidly growing branch of adaptive optics with applications such as light detection and ranging, imaging, optical communications, and atomic physics.

For spatial scanning of light, dielectric transparent matrices with variable refractive index with quantum dots can be used as active media, where the required phase delay is provided by a complex geometric distribution of quantum dots [1, 2]. Such systems are characterized by high speed and efficiency, however, their implementation requires state-of-the-art nanotechnology equipment.

Having high birefringence, nematic liquid crystals (LC) [3] are also considered as promising materials for implementation of such tasks. They are easily controlled by low-voltage electric fields, can have quite large working regions.

In this work we discuss the beam steering technique by using the photo-patterned structures in a liquid crystal film as polarization diffraction gratings. To change the intensity of diffraction maxima, the light polarization is varied by an electro-optic retarder: planar liquid crystal cell with applied electric field.

Combining two sets of the retarder and diffraction grating, we achieved a complex rearrangement of intensities of diffraction positions.

This work is supported by Higher Education and Science Committee of MESCS RA, project 21T-1C211.

### References

1. T. Piwonski et al. Refractive index dynamics of quantum dot based waveguide electroabsorbers. *Appl. Phys. Lett.* 97, 051107 (2010).
2. B. Çakır, Y. Yakar, and A. Özmen. Refractive index changes and absorption coefficients in a spherical quantum dot with parabolic potential. *J. Lumin.* 132, 2659–2664 (2012).
3. R. M. Matic. Blazed phased liquid crystal beam steering. *Proc. SPIE* 2120, 194–205, (1994).

## SC-DSB signal as a probe signal for testing nonlinearity in electronic circuits

N. Gasparyan<sup>1</sup>, A. Hakhoumian<sup>1,2</sup>, E. Sivolenko<sup>1</sup>, M. Barseghyan<sup>1</sup>

<sup>1</sup>*Yerevan State University, Alex Manoogian 1, Yerevan, Armenia*

<sup>2</sup>*Institute of Radiophysics and Electronics, Alikhanian Brothers str. 1, 0203 Ashtarak, Armenia*

Nowadays, there is a trend towards the widespread use of wireless devices for various applications, from data networks to wireless sensors. To find and characterize wireless devices, it is necessary to survey the surrounding environment. This becomes a problem when characterizing the properties of the RF circuit: when a two-dimensional signal is transmitted to an RF device, it is affected by nonlinear components of the circuit, amplifiers and diodes. Nonlinear components cause intermodulation distortion of the input signal, which is re-radiated by the device. The features of the intermodulation distortion result are used to build a fingerprint of the device. The fingerprint is then used to characterize the device so that it can be identified among other RF devices.

Keywords-RF Devices, Forensic Characterization, Intermodulation Distortion, Probe Signals, Circuit Models

### Acknowledgments

The work was supported by the Science Committee of RA, in the frames of the research project ԵՆ2023/2.

## Generation of THz pulses in the transparent ferromagnetic materials by optical rectification of ultrafast laser pulses

D. Baghdasaryan<sup>1</sup>, A. Makaryan<sup>1</sup>, V. Mekhitarian<sup>2</sup>, A. Poghosyan<sup>3</sup>, Y. Sahakyan<sup>1</sup>

<sup>1</sup>*Yerevan State University, Yerevan, 0025 Armenia,*

<sup>2</sup>*Institute for Physical Research, National Academy of Sciences of Armenia, Ashtarak2, 0203 Armenia*

<sup>3</sup>*University of Manchester, Oxford Road, Manchester M13 9PL, United Kingdom*

According to known experimental data (see for example [1]), a magnetized ferromagnetic medium exhibits magnetic nonlinearity  $B(H) = \mu_0 H + 4\pi \mu_0 \chi H + 4\pi M^{NL}(H)$ .

In the present work, the optical rectification of femtosecond laser radiation in a transparent ferromagnetic medium was investigated. The modeling of optical rectification in the COMSOL Multiphysics environment was performed.

It is shown that THz radiation can be generated by optical rectification of ultrafast laser pulses in the ferromagnetic material.

THz radiation in a monocrystalline YIG was experimentally obtained by optical rectification of femtosecond laser pulses in the infrared range. The magnitude of the THz signal depends essentially on the external magnetic field and the shape of the magnetization curve of the ferromagnetic sample.

This dependence is in good agreement with the static magnetization curve of the ferromagnetic sample. In the absence of an external magnetic field, the THz signal is also absent. The THz signal differs from zero at those values of the external magnetic field that correspond to the non-linear regions of the magnetization curve of the ferromagnetic sample.

[1] Martirosian, R.M., Makaryan, A.H., Mekhitarian, V.M., and Tadevosyan, V.R. Optical Detection in a Ferromagnet, JETP Letters. 2014. Vol. 99. No. 8. P. 435–440.

## Terahertz radiation in a nonlinear crystal partially filling a parallel-plate waveguide

A. S. Nikoghosyan<sup>1</sup>, V. R. Tadevosyan<sup>1</sup>, H. A. Parsamyan<sup>1</sup>, A. A. Poghosyan<sup>2</sup>.

<sup>1</sup>*Institute of Physics of Yerevan State University, Alek Manukyan str. 1, 0025 Yerevan, Armenia*

<sup>2</sup>*University of Manchester, Oxford Road, Manchester M13 9PL, United Kingdom.*

*nika@ysu.am*

This paper presents and explores a novel structure termed the “parallel plate nonlinear waveguide” (PPNW). A terahertz (THz) pulse is remotely excited in a PPNW antenna using femtosecond Ti Sapphire laser pulses. The terahertz radiation is generated by the optical rectification of a laser pulse in a nonlinear crystal that partially fills the cross-section of the waveguide. Nonlinear crystals such as LiNbO<sub>3</sub>, DAST, and GaSe are considered as efficient nonlinear frequency converters. For various applications, the propagation of the THz pulse in the waveguide in the form of the fundamental mode is of crucial importance.

The mode composition of a broadband THz pulse in the frequency range of 0.1–2.5 THz (represented as a linear superposition of coupled propagating TE<sub>n0</sub> modes, where n is an odd integer) in a nonlinear plate located in the middle of a waveguide with parallel metallic plates is investigated.

It has been shown that with a decreasing thickness of the nonlinear plate in PPNW, the frequency band in the spectrum of the terahertz pulse propagating in a waveguide as the fundamental single TE<sub>10</sub> mode increases. In particular, in a GaSe crystal with a thickness of 0.3 mm, the spectral components of the THz pulse from 200 GHz to 410 GHz, and in the case of a thickness of 0.08 mm, from 720 GHz to 1.5 THz, propagate as the TE<sub>10</sub> mode.

The results of experimental and numerical studies demonstrate that by adjusting the dimensions of the waveguide cross-section, the nonlinear crystal's dielectric susceptibility, and the position of the crystal within the waveguide cross-section, it is possible to modify the mode composition of the terahertz pulse. This allows for its propagation as the fundamental TE<sub>10</sub> mode or as a combination of modes such as TE<sub>10</sub> + TE<sub>30</sub>.

## Existing radio sources for antenna measurements

A. G. Ghulyan, N. D. Yezakyan, H. Arakelyan

*Institute of Radiophysics and Electronics, Alikhanian Brothers str. 1, 0203 Ashtarak, Armenia*

The most effective method for measurement of antenna parameters is radio astronomy method. In contrast to other methods, here is used cosmic communication and radio sources are located in cosmic space.

Conventional methods for measuring antenna parameters based on the use of ground-based transceivers and receivers, turn out to be insufficient, and in some cases, unrealizable. Due to the advent of large antennas and low-noise receiving devices, the requirements were increased for measuring parameters of antenna, such as noise temperature, dissipation coefficient, orientation diagram and effective square. Measuring these parameters of antenna with ground-based methods are impossible in practice.

The development of antenna technique has led to the need to research new methods for studying antenna parameters. Radioastronomy methods are such methods for measuring antenna parameters which are currently successfully used in antenna measurements. In practice, radioastronomy methods for measuring parameters of large antenna compared to ground-based methods is indisputable. Measurement of antenna properties in qualitative and control stability of system during operation are mandatory procedures.

Keywords: Antenna, radiometer, radio source, effective square, flux density, measurement.

## Design and Analysis of Quadcopter Classical Controller

N.D. Yezakyan

*Institute of Radiophysics and Electronics, Alikhanian Brothers str. 1, 0203 Ashtarak, Armenia*

Unmanned aerial vehicles (UAVs) are becoming more and more popular in a wide field of applications nowadays. In the work we have research existing types of UAVs. From these UAVs have chosen Quadcopter and developed control system (Figure 1). Main purpose of the work is to study the control system designing of UAVs. The study is viewing in different aspects: the designing of device, software and programming environments and controlling algorithms.

Keywords: drone, UAV, Quadcopter, Arduino, PCB.

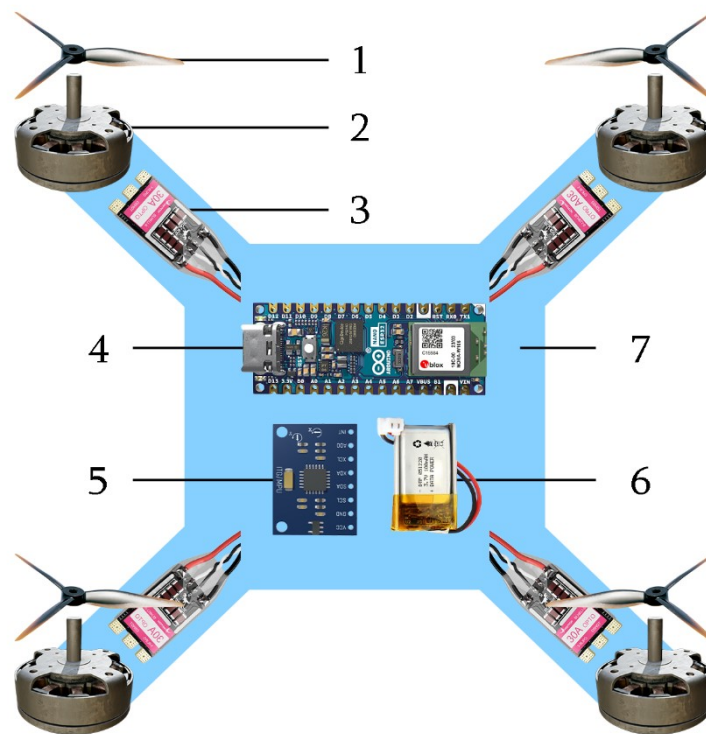


*Figure 1. Quadcopter parts*

## Tunable terahertz bandstop filter based on bilayer metasurface

L. Gevorgyan

*Yerevan State University, Alex Manoogian 1, Yerevan, Armenia*

Due to various applications, the Terahertz wave has attracted significant attention over the past two decades [1]. In recent years, 6G communication based on terahertz waves has attracted widespread attention [2]. Metasurface devices have demonstrated powerful capabilities of electromagnetic wave manipulation [3]. By adjusting the shape and size parameters of the metastructure, the resonance between spatial electromagnetic waves of the metasurface can be easily controlled, as a result control the structure's transmission, reflection, and absorption features.

In this work, we demonstrate through simulation calculations that a bilayer metasurface(BMS) composed of conductive rods can effectively function as a band stop filter in the terahertz frequency range (see Fig.1 a). The transmittance in the 0.6–0.9 THz range is approximately 2% or less, which implies a bandwidth of 0.3 THz and a center frequency of 0.75 THz (see Fig.1 b).

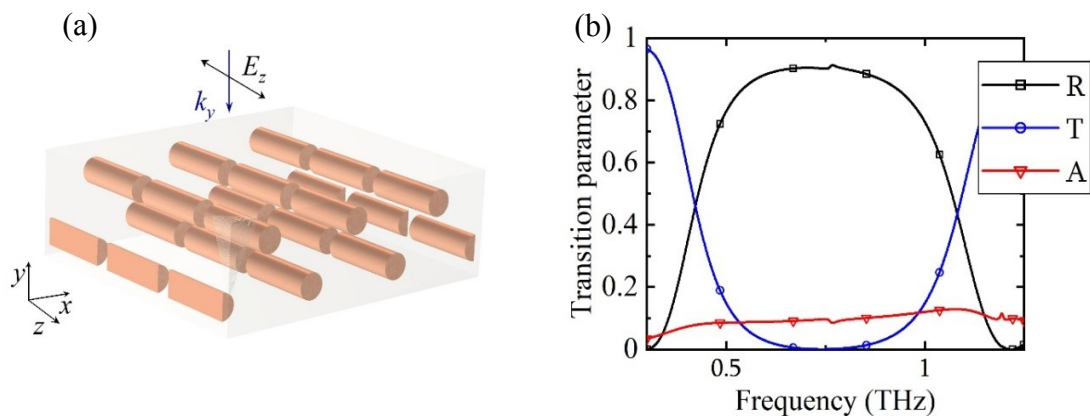


Fig. 1. (a) The schematic of the bilayer metasurface. (b) Transmittance, reflectance and absorptance spectra of the bilayer metasurface

The characteristics (bandwidth, central frequency, transition band and etc.) of proposed structure can be finely tuned by altering its geometric parameters, such as the diameter and length of rods, the periodicity, and the distance between the layers. The developed terahertz filter may have significant potential for applications in terahertz communications, sensors, and other emerging terahertz technologies.

### References:

1. Redo-Sanchez, A., Laman, N., Schulkin, B. *et al.* Review of Terahertz Technology Readiness Assessment and Applications. *J Infrared MilliTerahzWaves* 34, 500–518 (2013). <https://doi.org/10.1007/s10762-013-9998-y>
2. Rogalski, A. and Sizov, F.. "Terahertz detectors and focal plane arrays" *Opto-Electronics Review*, vol. 19, no. 3, 2011, pp. 346-404. <https://doi.org/10.2478/s11772-011-0033-3>
3. Xiaofei Zang, Bingshuang Yao, Lin Chen, Jingya Xie, Xuguang Guo, Alexei V. Balakin, Alexander P. Shkurinov, Songlin Zhuang. Metasurfaces for manipulating terahertz waves. *Light: Advanced Manufacturing* 2, 10(2021). [doi: 10.37188/lam.2021.010](https://doi.org/10.37188/lam.2021.010)

## **Spectral emission mask measurement improvement technique for IEEE 802.15.4z ultra-wideband devices**

Grigor Tsaturyan

*Institute of Information and Telecommunication Technologies and Electronics,  
National Polytechnic University of Armenia, Yerevan, Armenia*

The adoption of IEEE 802.15.4z ultra-wideband (UWB) technology is rapidly increasing due to its capabilities in delivering precise ranging, low latency, and interference-resistant communication for indoor navigation and centimeter-level distance determination applications. This growing usage has intensified the demand for accurate testing methods, especially to ensure compliance with spectral emission masks (SEM), which are critical for minimizing interference and ensuring reliable performance. Traditionally, SEM measurements have been conducted using a single signal analyzer, where the noise introduced by the analyzer itself can limit the accuracy of the results.

In this article, a novel approach for SEM measurement of 802.15.4z UWB waveforms is proposed, utilizing two synchronized signal analyzers combined with a cross-correlation technique. By cross correlating the received signals from both analyzers, the impact of analyzer noise is effectively mitigated, leading to a reduction in the noise of the measurement system. This approach enhances the precision of SEM measurements, ensuring that the spectral characteristics of the UWB waveform are accurately captured. A comparison of this method with traditional single-analyzer techniques is also presented.

Keywords - UWB technology, IEEE 802.15.4z, spectral emission mask measurements, synchronization of signal analyzers, spectral measurements, cross correlation.

## System design and implementation of multiprobe near field antenna measurements

Samvel Antonyan

*Institute of Information and Telecommunication Technologies and  
Electronics, National Polytechnic University of Armenia, Yerevan, Armenia*

This article presents practical implementation of a novel multiprobe planar near-field range (PNFR) measurement system, utilizing a simplified mechanical setup with four antipodal Vivaldi antennas serving as probes. The proposed system retains the design simplicity of existing configurations while enhancing measurement efficiency by reducing testing time. The antipodal Vivaldi antennas, known for their broadband capabilities, ensure precise and wideband near-field measurements. The developed setup is experimentally validated on a representative antenna under test (AUT) in the X-band frequency range, demonstrating its practical effectiveness and robustness in real-world applications. The results confirm system's ability to deliver high-resolution measurements, consistent with numerical simulations, thereby affirming its viability for advanced antenna testing and characterization.

Keywords - multiprobe planar near field antenna measurements, microstrip patch antenna characterization, antipodal Vivaldi antenna, planar near field antenna range, PNFR, multiprobe PNFR measurements.

## **Moving target indication as a radar cross section rapid estimate**

H.L. Babayan, N.G. Poghosyan, S.T. Sargsyan, T.V. Zakaryan \*

*Institute of Radiophysics and Electronics, Armenian National Academy of Sciences*

*Alikhanian 1, Ashtarak 0204, Armenia*

*\* tigr@irphe.am*

An alternate method for measuring the radar cross section (RCS) of objects without relying on expensive anechoic chambers to eliminate reflections from foreign objects is proposed. In traditional radar systems, reflections from stationary objects or clutter can indeed interfere with the desired signal. The distinguishing method is based on the well-established principle of moving targets indication (MTI). By exploiting the Doppler shift we are able to filter out reflections from stationary objects, which can significantly improve the accuracy of RCS measurements, which makes it possible to effectively extract a useful signal from a uniformly moving target under test. Reflections from stationary objects can be eliminated if we place the measured object on a uniformly moving at a certain speed platform. The use of higher-order MTI filters allows for even better clutter suppression, in environments with multiple stationary objects are present.

**Semiconductor and dielectric materials,  
electronic and optoelectronic devices  
(EL)**

## CdS thin films formed on flexible plastic substrate by low-temperature chemical bath deposition

S. Petrosyan<sup>1</sup>, A. Musayelyan<sup>1</sup>, A. Tokmajyan<sup>1</sup>, V. Gremenok<sup>2</sup>

<sup>1</sup>*Institute of Radiophysics and Electronics, NAS Armenia, 0203 Ashtarak, Armenia*

<sup>2</sup>*Scientific-Practical Materials Research Centre of the National Academy of Sciences of Belarus, 220072, Minsk, Petrus Brovka str., 19, of. 5, Belarus*

Polycrystalline cadmium sulfide (CdS) thin films were deposited onto polyimide (PI) plastic substrate by chemical bath technique at fixed solution temperature ( $62 \pm 1$ ) °C. We report the effect of deposition time on the structural and optical properties of as deposited thin films. Characterization of structural properties was carried out by X-ray diffraction (XRD). The XRD results confirmed that the deposited films are mainly consisting of hexagonal CdS phase and the crystallite size was about 10 nm and slightly decreased with deposition time. The root mean square roughness of the films was measured by atomic force microscopy. SEM micrographs show homogeneous, compact and smooth surface. The Raman multi-LO phonon modes we observed are characteristic for wurtzite structure CdS. The optical analyses based on the UV-Visible measurements, performed on the films deposited on flexible substrates, reveal the highest transmittance (~85%) and low reflectance (4-7)% in the wavelengths (520-1000) nm, with the optical band gap values of CdS films slightly increased as the deposition time increases, and it was found to be in the range of 2.3-2.36 eV. The photoluminescence spectrum of each CdS film shows two emission peaks located at 520 nm (2.4 eV) and 708 nm (1.75 eV) at room temperature, which may be attributed, respectively, to the free carrier recombination, excitonic transitions, donor-acceptor (DA) pairs recombination and donor levels-valence band (DL-VB) or conduction band-acceptor levels (CB-AL) radiative transitions.

The results demonstrate that the direct deposition of CdS from chemical bath on flexible PI substrates at the low temperature without the need any post-deposition treatment can result in improved physical properties of the films and paves the way to integrate CdS thin films in flexible optoelectronic devices.

## Differential thermal analysis of the crystallization kinetics in perlite-based nanocrystalline glass-ceramics

P. G. Petrosyan<sup>1</sup>, L.N. Grigoryan<sup>1</sup>, L. V. Asryan<sup>2</sup>, N. B. Knyazyan<sup>3</sup>, S. G. Petrosyan<sup>4</sup>

<sup>1</sup>*Institute of Physics, Yerevan State University, Yerevan, 0025, Republic of Armenia*

<sup>2</sup>*Department of Materials Science and Engineering, Virginia Polytechnic Institute and State University, Blacksburg, VA 24061, USA*

<sup>3</sup>*M.G. Manvelyan Institute of General and Inorganic Chemistry of the National Academy of Sciences, 0051, Republic of Armenia*

<sup>4</sup>*Institute of Radiophysics and Electronics of the National Academy of Sciences, Ashtarak, 0203, Republic of Armenia*

A glass-ceramic material containing nanosized crystallites synthesized based on the natural volcanic material perlite. Using the differential thermal analysis (DTA) method, the effect of  $\text{Na}_2\text{SiF}_6$  (a crystallization catalyst from the fluoride group) on the glass crystallization properties is studied. The characteristic glass-transition temperature  $T_g$ , peak crystallization temperature  $T_p$ , as well as the crystallization activation energy ( $E_c$ ) and Avrami index ( $n$ ) are determined in terms of the catalyst content in the initial composition. A decrease in the nucleation agent content is shown to increase  $T_g$ ,  $T_p$ , and  $E_c$ . The effect of the crystallization catalyst content on the crystallization mechanism and glass mechanical properties is discussed.

As the catalyst content decreases from 7% to 3%, the crystallization activation energy increases from 176 to 289 kJ/mol, while the Avrami parameter decreases from 3.82 to 2.83, confirming the change of the crystallization mechanism from three-dimensional crystal growth to the surface crystallization. The mechanical strength of the glass ceramics increases from 180 to 900 MPa and the Vickers microhardness from 7 to 9 GPa as the crystallization catalyst fraction increases from 3 to 7%.

## Bi-layer $\text{MoS}_2$ phototransistor deposited on a flexible substrate

S.G. Petrosyan<sup>1</sup>, A. M. Khachatryan<sup>1</sup>, P.G. Petrosyan<sup>2</sup>

<sup>1</sup>*Institute of Radiophysics and Electronics, NAS Armenia, Ashtarak, Armenia*

<sup>2</sup>*Institute of Physics, Yerevan State University, Yerevan, Armenia*

Using pulsed-laser deposition method a new phototransistor based on bi-layer  $\text{MoS}_2$  has been directly fabricated on polyamide (PI) substrate. Photocurrent generated under laser illumination in a top gate flexible FET is determined by illumination power for given drain and gate voltages. By controlling the gate and drain voltages the photo-responsivity can be tuned in a wide range. The photocurrent value solely depends on illumination intensity at constant drain and gate voltages. The structure shows the responsivity more than 12.5 mA/W. As a response to the pulsed illumination the structure shows a switching behavior with characteristic time in order of tens of ms. Such prompt photo-switching behavior, controllable by the incident light, exhibits stable characteristics. We observe a pronounced change in photocurrent value due to bending-induced strain variation of the band-gap. This observation supports a view of strain engineering as an enabling tool to fabricate new flexible devices based on few-layer  $\text{MoS}_2$  deposited on PI substrate. Among the potential applications of such  $\text{MoS}_2$  few-layer FET structure are nanoscale stress sensors and tunable photodetectors.

## Stoichiometry and phase composition of CdTe thin films prepared by pulsed laser deposition method

Khachatryan A.M.<sup>1</sup>, Petrosyan S.G.<sup>1</sup>, Hovsepyan B.L.<sup>1</sup>, Stanchik A.V.<sup>2</sup>

<sup>1</sup>*Institute of Radiophysics and Electronics of the National Academy of Sciences of Armenia, 0203 Ashtarak, st. Brothers Alikhanyan 1, Republic of Armenia*

<sup>2</sup>*“Scientific and Practical Center of the National Academy of Sciences of Belarus for Materials Science”, 200072 Minsk, st. P. Brovki 19, Republic of Belarus*

Cadmium telluride (CdTe) is one of the most promising materials for the manufacture of photocells, radioactive radiation detectors, thin film heterostructures Si/CdTe, CdTe/CdS and InSb/CdTe, which are actively used for solar cells and infrared photo detectors in the mid-infrared wavelength range of 3–5  $\mu\text{m}$ .

The purpose of this work is to study the elemental and phase composition, crystal structure of thin films of CdTe n-type conductivity, obtained by low-temperature laser pulse deposition on glass substrates.

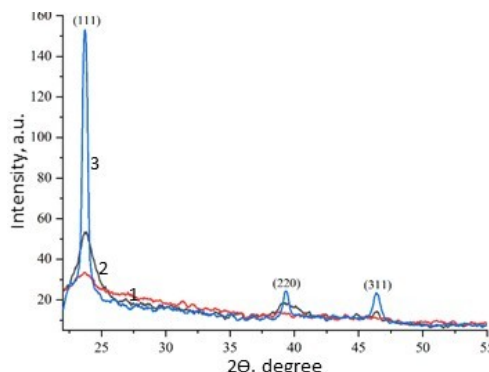
CdTe films were deposited on polished glass substrates using a laser wavelength of 1064 nm and a substrate temperature of 20 °C. During film deposition, the laser power was varied from 0.15 to 0.35 J, and the distance between the target and the substrate was changed from 30 to 50 mm. The study of the elemental composition of the samples was carried out by X-ray energy-dispersive microanalysis using a ZEISSEVO series scanning electron microscope. X-ray diffraction patterns of the samples were obtained using a DRON-3M X-ray diffractometer with CuK $\alpha$  radiation.

The table presents data on the elemental composition of thin CdTe films deposited on a glass substrate at a temperature of 20 °C, depending on the laser pulse energy and the distance from the target to the substrate. It can be seen that the composition of all the resulting CdTe films is close to stoichiometric one with a slight deviation towards an enrichment of Cd and, accordingly, a decrease in Te - no more than 2 at.% and 5 wt.%. It has been established that an increase in the laser pulse energy and the distance between the target and the substrate in the studied ranges does not lead to a change in the content of Cd and Te in the composition of the films within the error limits of the measurements (0.1%).

From the analysis of the X-ray diffraction patterns of thin CdTe films presented in the figure, it was established that all samples of CdTe films are single-phase. The diffraction patterns contain peaks at  $2\theta$  equal to 23.7, 39.3 and 46.6°, which correspond to the (111), (220) and (311) planes, respectively, of the cubic phase CdTe space group F  $\bar{4}3m$  (PDF#65-1081). The growth of CdTe films for all samples occurred predominantly in the (111) orientation, which corresponds to the CdTe cubic lattice.

*Table: Elemental composition of thin CdTe films depending on the laser power and the distance between the target and the substrate*

Sample №	P, J	L, mm	$\lambda$ , nm	Elemental composition			
				Cd		Te	
				at. %	wt. %	at. %	wt. %
3	0,15	30	1064	51,8	54,9	48,2	45,1
2	0,35	30		51,9	55,0	48,1	45,0
1	0,35	50		51,8	54,9	48,2	45,1



*X-ray diffraction patterns of thin CdTe films deposited at a substrate temperature of 20 °C.*

For the resulting CdTe films, an increase in the intensity of the main and additional peaks is observed with increasing film thickness, which is associated with an improvement in the crystallinity of the film. CdTe films obtained at a laser power of 0.15 J and a distance between the target and the substrate of 30 mm are characterized by the best crystallinity.

**Experimental determination of the binding energy  
of excitons in organometallic perovskite films  
 $\text{CH}_3\text{NH}_3\text{PbCl}_{3-x}\text{I}_x$  obtained by dual source vacuum  
thermal evaporation**

G. Ayvazyan<sup>1</sup>, H. Dashtoyan<sup>1</sup>, F. Gasparyan<sup>2</sup>, S. Khudaverdyan<sup>1</sup>, L. Matevosyan<sup>3</sup>

<sup>1</sup>National Polytechnic University of Armenia, Teryan str. 105, 0009 Yerevan, Armenia

<sup>2</sup>Yerevan State University, Alex Manoogian str. 1, 0025 Yerevan, Armenia

<sup>3</sup>Institute of Radiophysics and Electronics, Alikhanian Brothers str. 1, 0203 Ashtarak, Armenia

Organic and inorganic perovskites are promising semiconductor materials for manufacturing cheap and efficient solar cells, emitting diodes, photodetectors for visible and ultraviolet ranges, X-ray detectors, etc. Unique optical properties perovskites made it possible to increase the solar energy conversion coefficient from several percent to record values in a very short time. Despite the presence of a huge number of works on studying the properties of perovskites, many questions remain unanswered.

The most important parameter to consider when designing perovskite solar cells is the exciton binding energy. For efficient operation of a solar converter, it is necessary that at the operating temperature, most of the excitons dissociate into free electrons and holes, which could participate in the transfer of free charges. It is assumed that perovskites contain excitons with weak coupling, known as Wannier–Mott excitons. The binding energy for the  $n$ -th exciton level is described by the formula:  $E_n = E_g - R^*/n^2$  [1], where  $E_g$  is the band gap, and  $R^*$  is the effective Rietberg constant,  $R^* = R_0 \cdot m^*/m_0 \cdot \epsilon^2$  ( $R_0 = 13.6\text{eV}$ ),  $m^*$  is the reduced effective exciton mass ( $1/m^* = 1/m_e + 1/m_h$ ),  $m_e$  and  $m_h$  are the effective masses of electrons and holes (for metal-organic halogen perovskites  $m^* = 0.104 m_0$  [2]),  $m_0$  is the mass of a free electron, and  $\epsilon$  is the dielectric constant of the crystal. The calculated values of exciton binding energy in perovskites have a large scatter (from several meV to almost 50 meV), which is due to the large difference between the static and high-frequency dielectric constants of perovskites. Experimental values of exciton binding energy determined from absorption spectra performed at low temperatures also have a large scatter (from 5 meV to almost 100 meV). We also carried out research to experimentally determine the value of the exciton binding energy for a perovskite film of the composition  $\text{CH}_3\text{NH}_3\text{PbCl}_{3-x}\text{I}_x$ . Film synthesis was carried out in a vacuum chamber at a residual gas pressure of  $\sim 10^{-5}$  Torr. Evaporation was carried out from resistively heated quartz crucibles powered by independent sources. Inorganic lead iodide ( $\text{PbI}_2$ ) and organic methyl ammonium chloride ( $\text{CH}_3\text{NH}_3\text{Cl}$ , MACl) were used as precursors. Two types of samples were obtained: a perovskite film on a glass substrate and a perovskite film on a glass substrate pre-coated with FTO and  $\text{TiO}_2$  films. Optical spectroscopy was used to determine the exciton binding energy in the temperature range 300 – 77 K. Studies have shown that with decreasing temperature the absorption edge of films shifts to shorter wavelengths, and in the graphs at  $T < 100$  K the absorption peak of the first exciton level gradually stands out. The graphically determined values of the binding energy for both samples were about 14 meV, which is 12 meV less than the thermal activation energy at room temperature. Excitons with such a binding energy value at the operating temperature of the solar cell are highly likely to be destroyed and will participate in transfer mechanisms as a free electron and hole.

The study was carried out with the financial support of the Science Committee of the Republic Armenia within the framework of the scientific project no. 21AG-2B011.

1. M. Baranowski and P. Plachocka, Excitons in Metal-Halide Perovskites *Adv. Energy Matter.* 2020, 10, 1903659.
2. Miyata, A. Mitioglu, P. Plachocka, O. Portugall, H. Snaite et. al., Direct measurement of the exciton binding energy and effective masses for charge carriers in organic – inorganic tri – halide perovskites, *Nature Physics* 11(7), pp.582 – 587, 2015.

## Investigation of structural and optical properties of CsPbBr<sub>3</sub> films synthesized by single-source vacuum evaporation method

V. Harutyunyan<sup>1</sup>, L. Matevosyan<sup>2</sup>, V. Mkrtchyan<sup>1</sup>, G. Pluzyan<sup>2</sup>, S. Petrosyan<sup>1</sup>, A. Tokmajyan<sup>2</sup>

<sup>1</sup>Laboratory of Solid State Physics, Research Institute of Physics, Yerevan State University, A. Manukyan str. 1, 0025 Yerevan, Armenia

<sup>2</sup>Institute of Radiophysics and Electronics, Alikhanian Brothers str. 1, 0203 Ashtarak, Armenia

In recent years, there is a growing interest with respect to synthesis and investigation of physical and chemical properties of CsPbBr<sub>3</sub> perovskite polycrystalline films for their applications in solar cells, light-emitting diodes, photo detectors and other type devices [1]. These applications are stimulated by a high stability of CsPbBr<sub>3</sub> perovskite films against ambient humidity, high temperatures, and ultraviolet radiation. Amongst different synthesis/deposition techniques of CsPbBr<sub>3</sub> films: spin coating, vacuum thermal evaporation (VTE), atomic layer deposition, chemical vapor deposition, dip coating, and other mixed technologies. The vacuum evaporation from single or dual sources has some technological advantages and enables to deposit films at large areas, with uniform thickness, good flatness, and very importantly, without pores. Despite the large number of literature reports on the optical properties of polycrystalline CsPbBr<sub>3</sub> films deposited by the VTE method, it is still relevant to understand the changes in the optical properties of deposited films with time that occur after deposition process and to analyze these properties depending on the thermal annealing parameters (temperature and time) of the films.

This study investigated the optical characteristics (transmittance, reflectance, and absorbance) of CsPbBr<sub>3</sub> perovskite polycrystalline films deposited by VTE method. First, we investigated the stability of optical characteristics of as-deposited films under conditions of atmospheric environment and, next, it was analyzed the influence of the thermal annealing regime (temperature and time) on structural and optical characteristics of the films.

The CsPbBr<sub>3</sub> films were deposited onto pre-cleaned glass substrates with the use of equimolar amounts of PbBr<sub>2</sub> and CsBr precursors loaded into a common resistively heated quartz crucible (single-source evaporation approach). The investigations were conducted for film thicknesses in the range of 500 – 700 nm. The deposited films were subjected to thermal annealing in the temperature range of 250 – 350°C with a step of 25°C for annealing times of 15, 45, and 60 min at a fixed temperature. Structural and optical measurements were conducted by applying the X-ray diffraction, optical microscopy, and spectrophotometric techniques.

For all as-deposited samples, the recorded X-ray diffraction spectra show formation practically of pure CsPbBr<sub>3</sub> polycrystalline films with orthorhombic structure. After removal from the vacuum chamber, the optical transmittance (T) of the films in the range of strong absorption ( $\lambda < 530$  nm) undergoes a rapid change especially during the first two hours and stabilizes during two days. In this range ( $\lambda < 530$  nm), the films transform from semitransparent, T = (40–50)%, into almost completely absorbing, T = (4–6)%. In the long-wavelength range ( $\lambda > 530$  nm), the changes are insignificant, and the transmittance is T > (90 – 95)%.

For annealed CsPbBr<sub>3</sub> films, we observed the following trends in the grain morphology: (i) the annealing at temperature of 250°C preserves the grain sizes at submicron level, (ii) the annealing temperatures > 250°C result in formation of micron-sized grains  $\approx 2 - 15 \mu\text{m}$ , (iii) the annealing temperatures of 300°C (for annealing time of 60min) and 325°C (for all annealing times) cause sintering and further coarsening of grains, and (iv) at annealing temperature of 350°C and annealing time of 15min, the film loses its continuity and transforms into isolated islands. In films annealed at temperature of 325°C, we observed formation of pinholes with a high density. Besides, at annealing temperatures > 250°C, the CsPbBr<sub>3</sub> films exhibit formation of a strong texture along the crystallographic direction [100]. For optical absorbance of deposited films, it was obtained that with increase both of the annealing temperature and time the absorbance considerably decreases. From analysis of above presented results, we found the best regime of the thermal annealing for obtaining of coarse-grained CsPbBr<sub>3</sub> films with optimal optical characteristics.

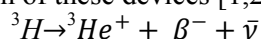
## Behavior of hydrogen, helium and their isotopes in silicon

V. Plotnikova, M. Nadahovskaya, E. Kalashnikov

*State University of Education. 105005, Moscow, Radio str., 10A, Russia*

Hydrogen and helium (and their isotopes) in silicon play an important role both at the stage of preparation of devices and during the operation of modern devices.

In particular, in betavoltaic devices the behavior of hydrogen atoms and its isotope - tritium  ${}^3\text{H}$  and helium isotope determines the operation of these devices [1,2]:



here  $\beta^-$  - beta particle,  $\bar{\nu}$  – antineutrino.

In this regard, we study the behavior of hydrogen, helium and their isotopes in silicon. In particular, it is shown that hydrogen, helium and their isotopes behave not as individual atoms with the corresponding masses, but as solitons with the corresponding effective masses [3,4]. The effective mass is determined by the mass of the atom itself and its polarizability. A soliton is a collective consisting of the atom itself (hydrogen, helium or their isotopes) and the accompanying reversible displacements of the nearest silicon atoms. At the same time, solitons of heavy isotopes move in silicon faster than solitons of light isotopes.

### **References**

1. T. Kostaski, N.P. Kherani, et al. Tritiated amorphous silicon betavoltaic devices. IEE Proc.-Circuits Devices Syst., Vol. 150, No. 4, August 2003. pp. 274-281.
2. T. Kostaski, N. P. Kherani, F. Gaspari. S. Zukotynski, W. T. Shmayda. Tritiated amorphous silicon films and devices. J. Vac. Sci. Technol. A 16.2., Mar/Apr 1998, pp.893-896.
3. V.I. Askerova, E.V. Kalashnikov. Movement of a Hydrogen Atom through Interstices in a Diamond-Like Lattice. *Defect and Diffusion Forum. Vol. 420, pp 162-171. 2022.*
4. Askerova V. I., Kalashnikov E. V. Effect of polarizability of a light atom (and its isotopes) on its movement in the form of a Frenkel–Kontorova soliton through a diamond-like lattice. In: *Bulletin of the Moscow Region State University. Series: Physics and Mathematics*, 2023, no. 2, pp. 20–28.

## The “untakeable” integral in electronic thin film science: calculated?

L. B. Hovakimian

*Institute of Radiophysics and Electronics of NAS RA, 0203 Ashtarak, Armenia*

In a classic study [1], where the notion of the celebrated Rytova-Keldysh interaction potential has been introduced, an integral representation was also obtained for a quasi-two-dimensionally screened Coulomb potential of a point charge in a thin film. The key role in this representation belongs to the parameter-dependent integral,  $I=I(r,\Lambda,R)$ , where  $r$  has the meaning of the in-plane distance from the point charge,  $\Lambda$  is the Rytova-Chaplik-Entin-Keldysh length scale, and  $R$  is the electronic screening radius [1, 2]. Much attention has been given over the years to the analysis of the screening physics described by  $I$  under the restrictive constraint  $\alpha\sim(\Lambda/R)\gg 1$ , due to which there is fundamentally no passage [1] to the limit of conducting plane from the film of a finite thickness. A conclusion has been reached that by virtue of this constraint the approximately calculated integral exhibits a  $\Lambda$ -insensitive structure,  $I\propto K_0(r/R)$  [2], where the zero-order Macdonald function,  $K_0(r/R)$ , shows an exponentially fast decaying tail in the far-field region,  $r/R\gg 1$ . An explanation of the physical reason for the origination of the exponential screening law in a thin film has also been given. The behavior of  $I$  counterpart in the electronic theory of topological insulator thin films was recently examined on the basis of numerical and asymptotic calculations in [3].

In this poster presentation the objective is to suggest a method for an analytical computation of the integral  $I(r,\Lambda,R)$  in the relevant case where the condition  $\alpha\geq 1$  is met. No evidence is found in our study that the physical information encapsulated in the screening integral is under control of the Macdonald function. Several features of phase shifted electrons in disordered quasi-two-dimensional systems are also discussed.

[1] N. S. Rytova, Moscow Univ. Phys. Bull. 3, 30 (1967).

[2] C. Huang *et al*, Nano Energy 41, 320 (2017).

[3] Yi Huang and B. I. Shklovskii, Phys. Rev. B 103, 165409 (2021).